

The following resources related to this article are available online at www.sciencemag.org (this information is current as of July 6, 2009):

Updated information and services, including high-resolution figures, can be found in the online version of this article at:

<http://www.sciencemag.org/cgi/content/full/324/5929/938>

Supporting Online Material can be found at:

<http://www.sciencemag.org/cgi/content/full/324/5929/938/DC1>

A list of selected additional articles on the Science Web sites **related to this article** can be found at:

<http://www.sciencemag.org/cgi/content/full/324/5929/938#related-content>

This article **cites 18 articles**, 12 of which can be accessed for free:

<http://www.sciencemag.org/cgi/content/full/324/5929/938#otherarticles>

This article has been **cited by** 1 articles hosted by HighWire Press; see:

<http://www.sciencemag.org/cgi/content/full/324/5929/938#otherarticles>

This article appears in the following **subject collections**:

Development

<http://www.sciencemag.org/cgi/collection/development>

Information about obtaining **reprints** of this article or about obtaining **permission to reproduce this article** in whole or in part can be found at:

<http://www.sciencemag.org/about/permissions.dtl>

which thousands of unmodified transposons may have been recruited for their transposase as part of the catalytic machinery of RNA-guided genome rearrangements just before they are eliminated from the macronuclear genome. In support of this model, we found that IES excision can precede transposon elimination (fig. S6), refuting a simple indirect effect of genome rearrangements occurring only after transposon processing. Transient TBE transposase expression begins after meiosis (Fig. 1 and fig. S1) and coincides with the production of maternal RNA templates that guide rearrangement (5) as well as all events of DNA processing, including TBE transposon elimination, IES excision, and segment-reordering in the developing nucleus (22).

References and Notes

1. D. M. Prescott, *Microbiol. Rev.* **58**, 233 (1994).
2. D. L. Chalker, M. C. Yao, *Mol. Cell. Biol.* **16**, 3658 (1996).
3. S. Duhaucourt, A. M. Keller, E. Meyer, *Mol. Cell. Biol.* **18**, 7075 (1998).

4. K. Mochizuki, N. A. Fine, T. Fujisawa, M. A. Gorovsky, *Cell* **110**, 689 (2002).
5. M. Nowacki *et al.*, *Nature* **451**, 153 (2008).
6. D. J. Witherspoon *et al.*, *Mol. Biol. Evol.* **14**, 696 (1997).
7. G. Herrick *et al.*, *Cell* **43**, 759 (1985).
8. T. G. Doak, F. P. Doerder, C. L. Jahn, G. Herrick, *Proc. Natl. Acad. Sci. U.S.A.* **91**, 942 (1994).
9. Single-letter abbreviations for the amino acid residues are as follows: A, Ala; C, Cys; D, Asp; E, Glu; F, Phe; G, Gly; H, His; I, Ile; K, Lys; L, Leu; M, Met; N, Asn; P, Pro; Q, Gln; R, Arg; S, Ser; T, Thr; V, Val; W, Trp; and Y, Tyr.
10. A. Seegmiller *et al.*, *Mol. Biol. Evol.* **13**, 1351 (1996).
11. K. Williams, T. G. Doak, G. Herrick, *EMBO J.* **12**, 4593 (1993).
12. L. A. Klobutcher, G. Herrick, *Prog. Nucleic Acid Res. Mol. Biol.* **56**, 1 (1997).
13. D. J. Hunter, K. Williams, S. Carinhour, G. Herrick, *Genes Dev.* **3**, 2101 (1989).
14. W. F. Doolittle, C. Sapienza, *Nature* **284**, 601 (1980).
15. L. E. Orgel, F. H. Crick, *Nature* **284**, 604 (1980).
16. T. G. Doak, D. J. Witherspoon, F. P. Doerder, K. Williams, G. Herrick, *Genetica* **101**, 75 (1997).
17. M. Morgante, P. De Paoli, S. Radovic, *Curr. Opin. Plant Biol.* **10**, 149 (2007).
18. M. G. Kidwell, A. J. Lish, *Evolution* **55**, 1 (2001).

19. V. V. Kapitonov, J. Jurka, *PLoS Biol.* **3**, e181 (2005).
20. A. Sarkar *et al.*, *Mol. Genet. Genomics* **270**, 173 (2003).
21. H. M. Robertson, K. L. Zumpano, *Gene* **205**, 203 (1997).
22. M. Möllenbeck *et al.*, *PLoS One* **3**, e2330 (2008).
23. Materials and methods are available as supporting material on Science Online.
24. This work was supported by NSF grant 0622112 and NIH grant GM59708. We thank J. Wang for technical assistance. DNA sequences have been deposited in GenBank under accession numbers FJ666213-FJ666314 (TBE transposases), FJ545743 [ribosomal DNA (rDNA) macronucleus], and FJ545744 (rDNA micronucleus).

Supporting Online Material

www.sciencemag.org/cgi/content/full/1170023/DC1

Materials and Methods

Figs. S1 to S6

Tables S1 to S4

References

DNA Sequence Data Files S1 to S8

19 December 2008; accepted 1 April 2009

Published online 16 April 2009;

10.1126/science.1170023

Include this information when citing this paper.

MAPK3/1 (ERK1/2) in Ovarian Granulosa Cells Are Essential for Female Fertility

Heng-Yu Fan,¹ Zhilin Liu,¹ Masayuki Shimada,² Esta Sterneck,³ Peter F. Johnson,⁴ Stephen M. Hedrick,⁵ JoAnne S. Richards^{1*}

A surge of luteinizing hormone (LH) from the pituitary gland triggers ovulation, oocyte maturation, and luteinization for successful reproduction in mammals. Because the signaling molecules RAS and ERK1/2 (extracellular signal-regulated kinases 1 and 2) are activated by an LH surge in granulosa cells of preovulatory follicles, we disrupted *Erk1/2* in mouse granulosa cells and provide in vivo evidence that these kinases are necessary for LH-induced oocyte resumption of meiosis, ovulation, and luteinization. In addition, biochemical analyses and selected disruption of the *Cebpb* gene in granulosa cells demonstrate that C/EBP β (CCAAT/Enhancer-binding protein- β) is a critical downstream mediator of ERK1/2 activation. Thus, ERK1/2 and C/EBP β constitute an in vivo LH-regulated signaling pathway that controls ovulation- and luteinization-related events.

In the mammalian ovary, the female germ cells (oocytes) reside within the ovarian follicles and are surrounded by somatic cell-derived granulosa cells (GCs) and cumulus cells that have endocrine functions and control oocyte maturation. Female reproductive success depends on the growth of ovarian follicles and differentiation of GCs as well as oocyte maturation and ovulation (1, 2). Although LH plays a critical role in the initiation of ovulation and in the terminal differentiation of GCs to luteal cells that compose the corpora lutea (CLs) and produce progesterone, the precise molecular targets in these processes remain ill-defined. Cyclic adenosine 3',5'-monophosphate (cAMP) is a well-known mediator of LH action, but LH also induces expression of the epidermal growth factor (EGF)-like factors that, via activation of the EGF receptor, RAS, and extracellular signal-regulated kinases 1 and 2 [ERK1/2, also known as mitogen-activated protein kinases 3 and 1 (MAPK3/1)], may act as the intrafollicular mediators to stimulate the cumulus cell-oocyte complex (COC) expansion and oocyte maturation (3–5). However, specific role(s) of the EGF network and, more specifically, of ERK1/2 in regulating ovulation, oocyte maturation, and the global reprogramming of GCs to luteal cells have not yet been analyzed or defined clearly in vivo.

ERK1 and ERK2 are coexpressed in all mammalian tissues and implicated as key regulators of cell proliferation and differentiation as well as oocyte maturation in culture (6, 7). Mutant mouse models have shown that *Erk1*-null mice are viable and fertile (8), but mutation of the *Erk2* gene is embryonic lethal in mice (9). To analyze the specific ovarian functions of ERK1 and ERK2 in vivo, we crossed *Erk2^{fl/fl}* mice (10) with the *Cyp19-Cre* transgenic mice (11), and the resultant *Erk2^{fl/fl};Cyp19-Cre* mice were further crossed into the *Erk1^{-/-}* background (8), yielding *Erk1^{-/-};Erk2^{fl/fl};Cyp19-Cre* (*Erk1/2^{sc-/-}*) mice. Efficient depletion of ERK1 and/or ERK2 in the mutant GCs and cumulus cells, as well as the lack of phosphorylation of ERK1/2 in the mutant GCs in vivo, was demonstrated (fig. S1, A to C). Loss of ERK1/2 did not impair LH-mediated activation of known upstream regulators of ERK1/2 or other LH-regulated signaling molecules (fig. S1, D and E) but did block phosphorylation of the ERK1/2 target RPS6KA2 (P90RSK) (fig. S1D).

The *Erk1^{-/-}* and *Erk2^{sc-/-}* females were fertile; however, the *Erk1/2^{sc-/-}* females failed to ovulate and were completely infertile (Fig. 1A). Ovaries of adult *Erk1/2^{sc-/-}* females contained preovulatory follicles but no CLs (fig. S2A). Concentrations of estradiol in serum were elevated (fig. S2B), causing constant vaginal estrus (fig. S2C). Even in immature *Erk1/2^{sc-/-}* females treated with exogenous hormones, events associated with ovulation did not occur: No oocytes matured, as indicated by the complete lack of germinal vesicle breakdown (GVBD) (Fig. 1A); no COCs expanded (Fig. 1, B and C, and fig. S2D); no follicles ruptured to form CLs (Fig. 1, D and E); and the concentration of estradiol in serum was elevated but that of progesterone was not (Fig. 1F), indicating profound endocrine changes in the mutant mouse ovaries. GCs in the equine chorionic gonado-

¹Department of Molecular and Cellular Biology, Baylor College of Medicine, 1 Baylor Plaza, Houston, TX 77030, USA.

²Department of Applied Animal Science, Graduate School of Biosphere Science, Hiroshima University, Higashi-Hiroshima, 739-8528, Japan. ³Laboratory of Cell and Developmental Signaling, Center for Cancer Research, National Cancer Institute-Frederick, Frederick, MD 21702–1201, USA. ⁴Basic Research Laboratory, Center for Cancer Research, National Cancer Institute-Frederick, Frederick, MD 21702–1201, USA. ⁵Molecular Biology Section, Division of Biological Sciences and Department of Cellular and Molecular Medicine, University of California, San Diego, La Jolla, CA 92093, USA.

*To whom correspondence should be addressed. E-mail: joanner@bcm.edu

tropin (eCG)-primed *Erk1/2^{gc-/-}* females were viable but exhibited signs of apoptosis when luteinization failed (fig. S2E).

Specific analyses of oocyte functions showed that oocytes isolated from the COCs of *Erk1/2^{gc-/-}* mutant mice spontaneously underwent GVBD in culture and progressed to metaphase II stage, as did controls (fig. S3A). By contrast, when spontaneous GVBD was blocked by hypothanxine (HX), the EGF-like factor amphiregulin (AREG) stimulated GVBD in wild-type (WT) but not *Erk1/2^{gc-/-}* COCs (fig. S3B). In addition, AREG stimulated expansion of COCs isolated from WT, but not the *Erk1/2^{gc-/-}* mice (fig. S3C). These results indicate that the oocytes that retain ERK1/2 in the *Erk1/2^{gc-/-}* mice are competent for meiotic maturation, but the cumulus cells lacking ERK1/2 (fig. S1B) fail to respond to EGF-like factors.

Furthermore, the ability of LH/hCG (human chorionic gonadotropin) to terminate GC proliferation was impaired in the *Erk1/2^{gc-/-}* mice, as indicated by elevated incorporation of bromodeoxyuridine (BrdU) (Fig. 2, A and B, and fig. S4, A and B) and expression of positive cell cycle-regulatory molecules CCND2, CCNA, and E2F1 and reduced expression of CDKN1B and CDKN1A (fig. S4, C and D) in the mutant ovaries compared to controls. Thus, ERK1/2 control GC fate decisions at this critical stage of their differentiation.

To identify ERK1/2 target genes in preovulatory follicles, we analyzed gene expression profiles using RNA prepared from GCs obtained from WT and *Erk1/2^{gc-/-}* mice treated with eCG for 48 hours and at 0, 2.5, and 4 hours after hCG injection because the activation of ERK1/2 peaks at 2 hours after hCG treatment (11, 12) and many genes that affect ovulation are maximally expressed by 4 hours (5). Among the 563 highly regulated LH target genes (more than fourfold, hCG at 4 hours versus hCG at 0 hours; 466 with increased and 97 with decreased expression, tables S1 and S2), 77% (376 with increased and 57 with decreased expression) lost their response to LH/hCG in the *Erk1/2^{gc-/-}* cells (Fig. 3A). Two identified ERK1/2 target genes that regulate estradiol biosynthesis and activity are *Cyp19a1* (aromatase), which converts testosterone to estradiol, and *Sult1e1*, which deactivates estradiol (13). Whereas hCG turns off *Cyp19a1* expression in WT mice, *Cyp19a1* was markedly increased in the *Erk1/2^{gc-/-}* cells. By contrast, hCG transiently induced *Sult1e1* in WT but not *Erk1/2^{gc-/-}* GCs (Fig. 3B and tables S1 and S2), leading to inappropriately high estradiol concentrations (Fig. 1F and fig. S2B) that may adversely affect the ovary and other tissues as well (13). Conversely, two luteinization markers, *Star* and *Cyp11a1*, were substantially reduced in the *Erk1/2^{gc-/-}* ovaries, consistent with the lack of CLs in the mutant mice (Fig. 2, C to F, and fig. S5, A and B).

The expression of many genes associated with COC expansion and ovulation (*Ptgs2*, *Tnfrsf6*, *Has2*, *Ptx3*, and *Pgr*) was abolished

in the *Erk1/2^{gc-/-}* ovaries, as indicated by the microarray data (table S1), quantitative reverse transcription-polymerase chain reaction (qRT-PCR) (Fig. 3C and fig. S5A), and immunoflu-

orescence (fig. S5D), whereas genes encoding the two EGF-like factors *Areg* and *Ereg*, presumed mediators of LH action, were induced rapidly to normal (*Ereg*) or reduced (*Areg*) levels compared

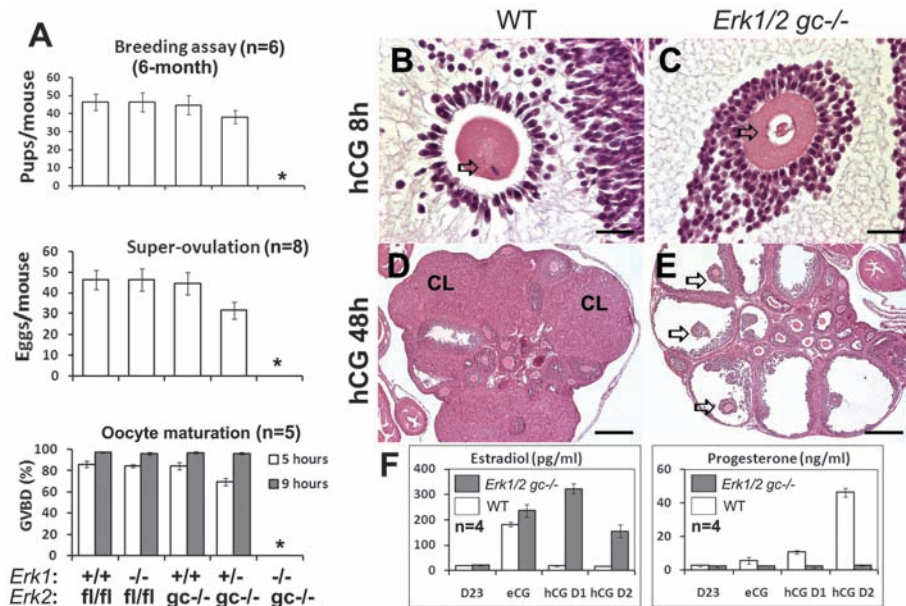
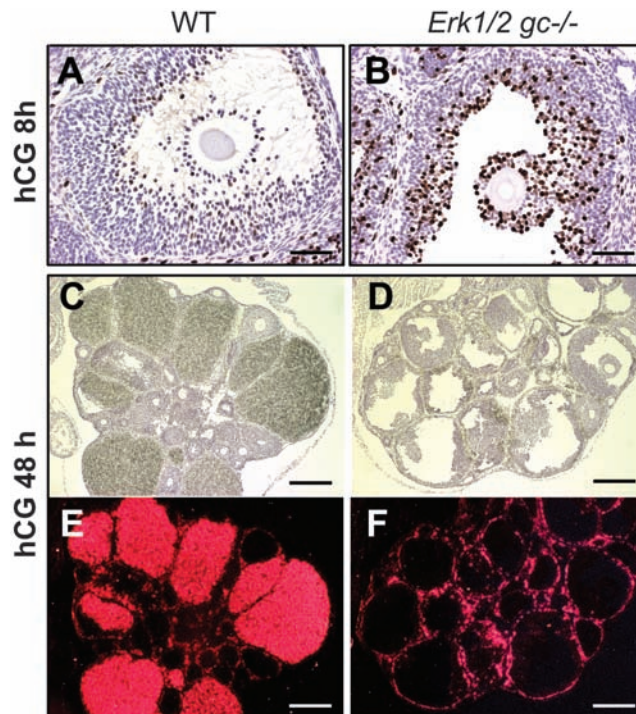


Fig. 1. ERK1/2 mediate LH-induced oocyte maturation, ovulation, and luteinization. (A) Breeding assays, superovulation assays, and oocyte maturation (germinal vesicle breakdown; GVBD) rate in the different mouse genotypes. An asterisk (*) indicates that the data point is zero. Error bars denote SD. (B to E) Hematoxylin and eosin (H&E) staining of ovaries from immature WT and *Erk1/2^{gc-/-}* mice treated with hCG for 8 hours (B and C) or 48 hours (D and E). CL: corpus luteum. In (B) and (C), arrows indicate the nuclear configuration of the oocyte nucleus. Scale bars, 31.25 μ m. In (D) and (E), arrows indicate nonovulated COCs in preovulatory follicles. Scale bars, 250 μ m. (F) Changes in estradiol and progesterone concentrations in serum after hCG treatment of eCG-primed 3-week-old WT and *Erk1/2^{gc-/-}* females. D23: postnatal day 23; eCG: 23-day-old female mice treated with eCG for 48 hours; hCG D1 and hCG D2: 23-day-old females treated with eCG for 48 hours followed by hCG for 24 hours (D1) or 48 hours (D2).

Fig. 2. ERK1/2 are required for the terminal differentiation of GCs during ovulation. (A and B) BrdU staining of WT and *Erk1/2^{gc-/-}* ovary sections at 8 hours after hCG treatment. Scale bars, 62.5 μ m. (C to F) In situ hybridization shows the expression of *Cyp11a1* mRNA in ovaries of WT and *Erk1/2^{gc-/-}* mice at 48 hours after hCG treatment. Histology of the ovaries is shown by hematoxylin staining (C and D); localization of *Cyp11a1* mRNA is shown by dark-field images (E and F). Scale bars, 250 μ m.



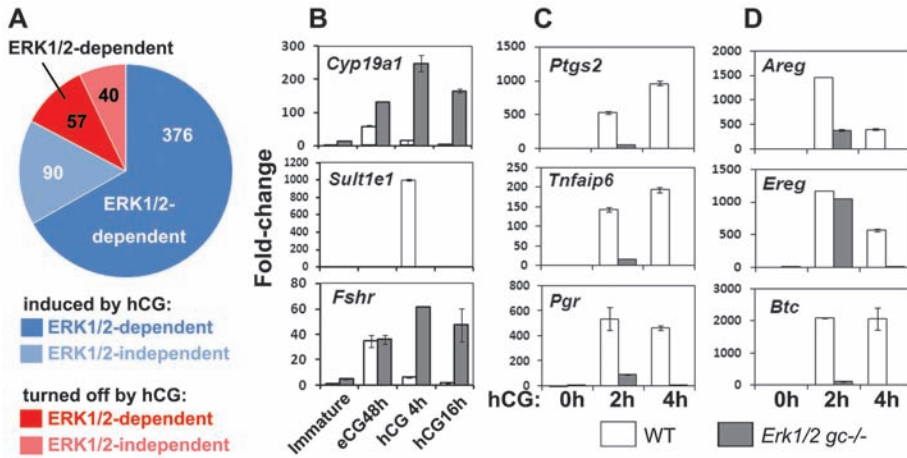


Fig. 3. ERK1/2 extensively regulate the expression of FSH/LH-target genes during ovulation. **(A)** Summary of gene expression profiling data. Genes regulated more than fourfold between 0 and 4 hours after hCG treatment were defined as LH-target genes; those that failed to respond to hCG in the *Erk1/2^{gc-/-}* cells were defined as ERK1/2-dependent genes. **(B to D)** qRT-PCR shows the expression of selected FSH/eCG and LH/hCG target genes in GCs of WT and *Erk1/2^{gc-/-}* mice after hCG treatment. Error bars denote SD.

to controls but these levels were not sustained. By contrast, the induction of betacellulin (*Btc*) was blocked completely in *Erk1/2^{gc-/-}* ovaries (Fig. 3D). Thus, the initial induction of *Areg* and *Ereg* by LH/hCG is largely independent of ERK1/2 activation. However, the induction of *Btc* and the secondary maintenance of *Areg* and *Ereg* expression is likely dependent on ERK1/2 induction of *Ptgs2*, leading to prostaglandin E2 (PGE2) production and activation of the EP2 receptor (5).

By contrast, genes in addition to *Cyp19a1* that are expressed and/or induced by follicle-stimulating hormone (FSH) and equine chorionic gonadotropin (eCG) in GCs during preovulatory follicle development (*Fshr*, *Lhcgr*, and *Nr5a2*) (fig. S6) and normally down-regulated during the early stages of LH-induced luteinization (*I4*) were expressed at elevated levels in ovaries of the hormone-treated *Erk1/2^{gc-/-}* mice (Fig. 3B and fig. S5C). Thus, ERK1/2 is required for suppressing the expression of FSH target genes.

Mice null for the transcription factor CCAAT/Enhancer-binding protein- β (*Cebpb*) are one of a only few knockout mouse models that show an *Erk1/2^{gc-/-}*-like ovarian phenotype (15). C/EBP β protein is increased rapidly by hCG in GCs in vivo (fig. S7, A and B), and in cultured cell lines. C/EBP β is the substrate of ERK1/2 and/or RPS6KA2 (P90RSK) (16), making C/EBP β a potential mediator of ERK1/2 in GCs. Indeed, when undifferentiated GCs were infected with an adenoviral vector encoding C/EBP β , C/EBP β was expressed, phosphorylated in response to AREG at a known ERK1/2 site and by a MEK1/2-dependent mechanism (C/EBP β -T188; Fig. 4A). Only in C/EBP β -expressing cells could AREG induce ERK1/2-dependent (U0126 sensitive) expression of target genes (*Ptgs2*, *Tnfaip6*, *Pgr*, and *Star*) (Fig. 4A and fig. S8A). AREG and C/EBP β induced the expression of LH/ERK1/2 target genes in *Erk1/2^{gc-/-}* GCs only when an ERK2 expression vector restored kinase activity (Fig. 4A). The synergistic actions of AREG and C/EBP β were compromised dramatically by an ERK1/2 site, but not P90RSK site, point mutation (fig. S8A), indicating that C/EBP β is a direct target of ERK1/2 and both constitute a critical signaling network in preovulatory GCs.

Because the GC-specific functions of C/EBP β have not been studied in vivo, *Cebpb^{fl/fl}* mice (17) were crossed with the *Cyp19-Cre* mice, generating the *Cebpb^{fl/fl};Cyp19-Cre* (*Cebpb^{gc-/-}*) mouse strain with C/EBP β depleted in GCs (fig. S7, B to D). As in the *Cebpb*-null mice (15), the adult *Cebpb^{gc-/-}* mice were subfertile (fig. S7E). CLs were absent in 70% of the adult *Cebpb^{gc-/-}* mice ($n = 10$, Fig. 4B); the number of ovulated COCs was reduced (Fig. 4C); and the expression of *Ptgs2*, *Star*, and *Cyp11a1* was decreased, consistent with impaired CL formation (fig. S7, F to G). However, hCG-induced phosphorylation of MEK1/2 and ERK1/2 was normal in ovaries of *Cebpb^{gc-/-}* mice (fig. S7D). Expression

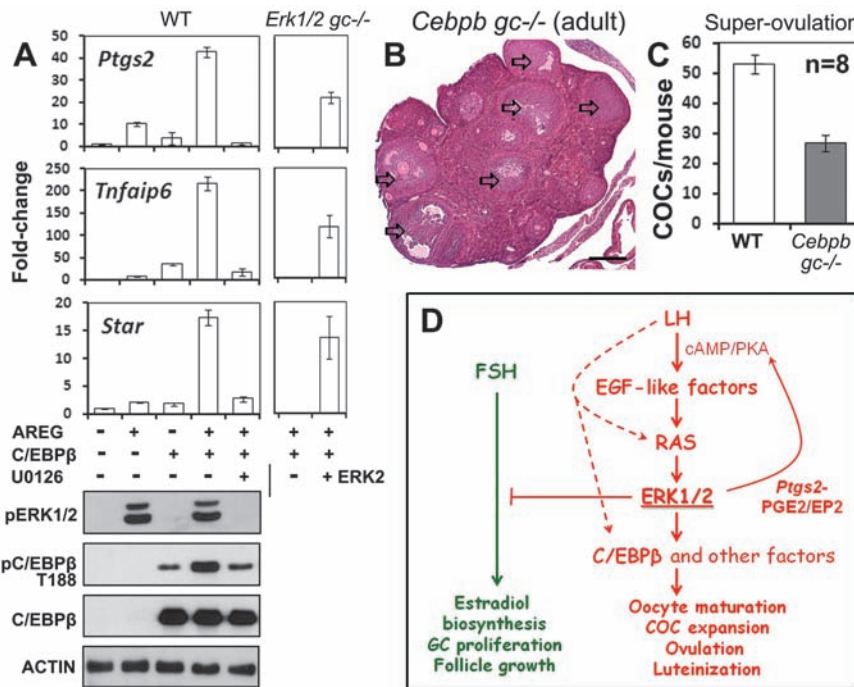


Fig. 4. C/EBP β is a key mediator of ERK1/2 activity in preovulatory GCs. **(A)** Immature WT or *Erk1/2^{gc-/-}* mice were primed with eCG for 24 hours. GCs were collected and cultured overnight, and some *Erk1/2^{gc-/-}* GCs were transfected with an ERK2 expression plasmid. The cells were then infected with an adenoviral vector encoding C/EBP β for 4 hours and further treated with AREG with (+) or without (-) U0126 for another 4 hours. Total RNA or protein was extracted. LH, hCG, and AREG downstream genes were quantified by qRT-PCR. Western blots document AREG-induced phosphorylation of ERK1/2 and C/EBP β and overexpression of C/EBP β . Error bars denote SD. **(B)** H&E staining shows the absence of CLs in the ovary of adult *Cebpb^{gc-/-}* mice. Follicles are indicated by arrows. Scale bar, 250 μ m. **(C)** The number of ovulated COCs decreased at 16 hours after hCG injection in *Cebpb^{gc-/-}* mice. **(D)** Summary. LH, cAMP, and protein kinase A (PKA) induce AREG and EREG, which activate RAS and ERK1/2. Activated ERK1/2 is required to (i) induce and activate CEBP β and genes essential for oocyte maturation, ovulation, and luteinization; (ii) maintain AREG, EREG, and BTC by inducing *Ptgs2*/PGE and activation of EP2, cAMP, and PKA; and (iii) silence the FSH-regulated program. LH may also transactivate RAS and ERK1/2 directly and regulate C/EBP β expression by other pathways. FSH and LH pathways are shown in green and red, respectively.

of C/EBP β was decreased but not totally blocked in the *Erk1/2^{gc-/-}* mice (fig. S8, B and C), indicating that C/EBP β expression is regulated by additional pathways and that ERK1/2-mediated phosphorylation and activation of C/EBP β is critical. Thus, C/EBP β is a downstream effector of ERK1/2 in GCs during ovulation and luteinization. The lower penetrance of ovulation and gene expression defects in *Cebpb^{gc-/-}* mice, compared with the *Erk1/2^{gc-/-}* mice, suggests that C/EBP β is one, but not the only, critical transcription factor regulated by ERK1/2 in vivo.

The *Erk1/2^{gc-/-}* mouse model illustrates that disruption of *Erk1/2* in GCs in vivo completely derails the ability of LH to induce genes controlling ovulation, COC expansion, oocyte maturation, and luteinization without altering genes that regulate normal follicular development to the preovulatory stage (summarized in Fig. 4D). As a consequence of ERK1/2 depletion in GCs, the FSH program is extended rather than being abruptly terminated by LH/hCG. Thus, our results demonstrate in animals that the critical roles of ERK1/2 in GCs are highly selective and cell context-specific, confirming findings of in vitro studies (6, 18). Moreover, ERK1/2 are activated for a relatively short period of time (from 0.5 to 2 hours) in GCs of the preovulatory follicles exposed to LH/hCG (11, 12, 19), and this brief window of activation is necessary and suf-

ficient to reprogram preovulatory GCs to cease dividing and terminally differentiate.

The effect of ERK1/2 activation in GCs of preovulatory follicles but not in follicles at earlier stages of growth indicates that activation of these kinases is controlled tightly by specific mechanisms. Indeed, inappropriate activation of ERK1/2 in GCs of small growing follicles might disrupt normal follicular development because mice in which ovarian GCs express a constitutively active K-RAS mutant suffer impaired follicle development and premature ovarian failure (11). Thus, further understanding of the molecular mechanisms by which ERK1/2 regulate ovarian cell functions will help unravel some of the causes of ovarian pathologies and cancer, as well as lead to therapies for female infertility.

References and Notes

1. M. Hunzicker-Dunn, E. T. Maizels, *Cell. Signal.* **18**, 1351 (2006).
2. M. M. Matzuk, K. H. Burns, M. M. Viveiros, J. J. Eppig, *Science* **296**, 2178 (2002).
3. J. Y. Park *et al.*, *Science* **303**, 682 (2004).
4. M. Hsieh *et al.*, *Mol. Cell. Biol.* **27**, 1914 (2007).
5. M. Shimada, I. Hernandez-Gonzalez, I. Gonzalez-Robayna, J. S. Richards, *Mol. Endocrinol.* **20**, 1352 (2006).
6. Y. Q. Su, K. Wigglesworth, F. L. Pendola, M. J. O'Brien, J. J. Eppig, *Endocrinology* **143**, 2221 (2002).
7. Z. Chen *et al.*, *Chem. Rev.* **101**, 2449 (2001).
8. G. Pages *et al.*, *Science* **286**, 1374 (1999).
9. M. Aouadi, B. Binetruy, L. Caron, Y. Le Marchand-Brustel, F. Bost, *Biochimie* **88**, 1091 (2006).

10. A. M. Fischer, C. D. Katayama, G. Pages, J. Pouyssegur, S. M. Hedrick, *Immunity* **23**, 431 (2005).
11. H. Y. Fan *et al.*, *Development* **135**, 2127 (2008).
12. S. Panigone, M. Hsieh, M. Fu, L. Persani, M. Conti, *Mol. Endocrinol.* **22**, 924 (2008).
13. E. Gershon, A. Hourvitz, S. Reikhav, E. Maman, N. Dekel, *FASEB J.* **21**, 1893 (2007).
14. J. S. Richards, *Endocrinology* **142**, 2184 (2001).
15. E. Sterneck, L. Tessarollo, P. F. Johnson, *Genes Dev.* **11**, 2153 (1997).
16. M. Bück, V. Poli, P. vander Geer, M. Chojkier, T. Hunter, *Mol. Cell* **4**, 1087 (1999).
17. E. Sterneck, S. Zhu, A. Ramirez, J. L. Jorcano, R. C. Smart, *Oncogene* **25**, 1272 (2006).
18. S. Sela-Abramovich, E. Chorev, D. Galiani, N. Dekel, *Endocrinology* **146**, 1236 (2005).
19. E. T. Maizels, J. Cottom, J. C. Jones, M. Hunzicker-Dunn, *Endocrinology* **139**, 3353 (1998).
20. We thank J. Pouyssegur and J. Shao for providing *Erk1^{-/-}* mice and adenoviral vector of C/EBP β , respectively. This work was supported by NIH grants NIH-HD16229, NIH-HD07495, Project II (J.S.R.), Grant-in-Aid for Scientific Research No. 18688016 from the Japan Society for the Promotion of Science (M.S.), Intramural Research Program of NIH, National Cancer Institute, Center for Cancer Research (P.F.J. and E.S.), and NIH Postdoctoral Training Grant NIH-HD07165 (H.-Y.F.). The Gene Expression Omnibus accession number for microarray data is GSE15135.

Supporting Online Material

www.sciencemag.org/cgi/content/full/324/5929/938/DC1
Materials and Methods
Figs. S1 to S8
Tables S1 and S2
References

26 January 2009; accepted 20 March 2009
10.1126/science.1171396

Cell Movements at Hensen's Node Establish Left/Right Asymmetric Gene Expression in the Chick

Jerome Gros,¹ Kerstin Feistel,^{2*} Christoph Viebahn,³ Martin Blum,² Clifford J. Tabin^{1†}

In vertebrates, the readily apparent left/right (L/R) anatomical asymmetries of the internal organs can be traced to molecular events initiated at or near the time of gastrulation. However, the earliest steps of this process do not seem to be universally conserved. In particular, how this axis is first defined in chicks has remained problematic. Here we show that asymmetric cell rearrangements take place within chick embryos, creating a leftward movement of cells around the node. It is the relative displacement of cells expressing *sonic hedgehog* (*Shh*) and *fibroblast growth factor 8* (*Fgf8*) that is responsible for establishing their asymmetric expression patterns. The creation of asymmetric expression domains as a passive effect of cell movements represents an alternative strategy for breaking L/R symmetry in gene activity.

In mice and rabbits, monocilia found on cells of the posterior notochordal plate have been shown to play a crucial role in breaking left/right (L/R) symmetry (1, 2). These cilia are able to create a leftward flow of fluid in a pit-like teardrop-shaped space that is not covered by subjacent endoderm (3). The flow of fluid across this pit stimulates signal transduction that ultimately leads to the induction of asymmetric gene expression (1, 2).

In contrast, in the chick embryo, the endoderm underlying Hensen's node (a structure at

the rostral end of the primitive streak in the gastrulating embryo) exists as a continuous sheet ventral to the notochordal plate mesoderm (4), and there is no morphological pit on the ventral surface in which a flow of fluid could be established. Essner *et al.* have observed cilia at Hensen's node in earlier work (5), but these short cilia are on endodermal cells and are unrelated to the motile cilia on the mesodermal cells of the ventral node in the mouse and rabbit. The mesodermal cells at Hensen's node in the chick are devoid of cilia. In addition, the Talpid chick

mutant lacks primary cilia (6) but does not exhibit L/R asymmetry defects. Unlike in the mouse and rabbit, the chick node itself becomes morphologically asymmetric, with a marked tilt toward the left around the time the primitive streak reaches full extension at stage 4 (7, 8) (Fig. 1, A to C). Shortly thereafter, a number of small L/R asymmetric expression domains are observed to the right and left of the node (9). However, all of the genes expressed in such a manner are initially expressed in a symmetric fashion: for example, *fibroblast growth factor 8* (*Fgf8*) bilaterally along the primitive streak and *sonic hedgehog* (*Shh*) bilaterally across the top of the node until stage 4 (10) (Fig. 1, D to G). Subsequently, concomitant with the development of morphological asymmetries in the node, these gene expression patterns also become gradually asymmetric by stage 5 (Fig. 1, H and I).

To investigate cellular rearrangements that could be responsible for establishing the morphological asymmetry of the node, we performed

¹Department of Genetics, Harvard Medical School, Boston, MA 02115, USA. ²Institute of Zoology, Hohenheim University, 70953 Stuttgart, Germany. ³Department of Anatomy and Embryology, Göttingen University, 37079 Göttingen, Germany.

*Present address: Division of Neuroscience, Oregon National Primate Research Center, Oregon Health and Science University, Beaverton, OR 97006, USA.

†To whom correspondence should be addressed. E-mail: tabin@genetics.med.harvard.edu